Rotational Coherence Measurements and Structure Calculations of Hydrogen-Bonded Complexes of Perylene with Water and Alcohols

Peter M. Andrews, Brian A. Pryor, Mitchell B. Berger, Phillip M. Palmer, and Michael R. Topp*

Department of Chemistry, University of Pennsylvania, Philadelphia, Pennsylvania 19104-6323

Received: May 20, 1997; In Final Form: July 1, 1997[⊗]

Rotational coherence spectroscopy has been used to measure the inertial properties of 1:1 complexes of perylene with water and several different aliphatic alcohols, under supersonic expansion conditions. Hole-burning experiments confirm that several complexes, including ethanol, 1-propanol, and 2-propanol, are present in at least two distinct structural forms. On the other hand, for the methanol and *tert*-butyl alcohol complexes, only a single structure was detected. The water complex also exists in two ground-state forms, but so far only one of these has been structurally identified. Structures calculated via molecular mechanics procedures, using the CVFF and CFF91 force fields and parameters from the Biosym protein database, are remarkably consistent with experimental inertial measurements. Some comparisons with other molecular mechanics procedures are also presented. We have determined that all these complexes involve a hydrogen bond to π-electrons in the outer rings of the aromatic molecule. The structural variants usually involve rotation about this bond site to different registry positions with the perylene aromatic rings, effectively conserving the alcohol geometry. However, one form of the 1-propanol complex may involve a *gauche* isomer of the alcohol molecule.

1. Introduction

The hydrogen bond plays an important role in many chemical and biological processes, ranging from the fundamental building blocks of proteins and nucleic acids to simple acid−base reactions. All species in contact with an aqueous solution, whether soluble or at an interface, have properties that are profoundly sensitive to the hydrogen-bonding nature of water. Apart from the bulk dielectric properties of hydrogen-bonding solvents, these specific interactions can strongly influence the energies of molecular electronic states, and site-specific interactions such as proton transfer often dominate molecular photochemical processes.

Molecular clusters generated under supersonic jet conditions provide an important means to examine the dependence of emergent "solvation" behavior on the number, composition, and, ideally, specific molecular arrangements of interacting molecules. Such clusters are naturally prepared at cryogenic temperatures and therefore exhibit highly resolved spectra. On the other hand, unlike cryogenic media, the molecular arrangement in clusters is weakly constrained, so that excess energy provided via laser irradiation can lead to facile structure relaxation. Moreover, a wide variety of "solvent−solute" combinations can be explored under these conditions.

Many experiments on clusters involving the aromatic molecule perylene have been coupled with structure calculations. Apart from the simplest cases, successful calculations on molecular clusters require consideration of the effects of charge separation. Some such studies have included calculations on the 1:1 complex of perylene with benzene, where the electrostatic interactions were modeled on the basis of distributed point charges[1] or distributed multipoles.[2] Also, Castella et al.[3] employed a "charge resonance" approach to calculate the structures of "donor−acceptor"-type complexes of perylene with benzene derivatives including phenol and aniline. However, at the time, those works did not have the benefit of experimental structure measurements for reference. Since the pioneering experiments by Felker and co-workers, applying rotational coherence spectroscopy to the perylene system,[4] and particularly the benzene complex,[5] it has been possible to calculate structures of van der Waals clusters with greater confidence.

Several cases have been identified where complexes at the 1:1 level appear in different structural forms, separated by small potential-energy barriers. Some examples have been demonstrated where vibrational energies ≤ 300 cm^{-1} can lead to barrier crossing and large-amplitude internal motion, resulting in the mixing or relaxation of structures. These include 1:1 complexes of perylene with alkyl halides[6,7] and *p*-dichlorobenzene,[8] and the 1:1 complex of coumarin 151 with water.[9] Such effects can be detected by observation on a picosecond time scale of fluorescence Stokes shifts following vibronic excitation. Successful predictions of the different types of structures and their relative stability will provide an important test of the reliability of computation techniques. However, these larger-molecule cases present important computational challenges in a regime (i.e., 30−50 atoms) where *ab initio* approaches are difficult to apply, and semiempirical quantum mechanical approaches often fail to reproduce experimental data. Molecular mechanics calculations, although less precise than the above, can play an important role in structure predictions for these large systems.

"Classical" hydrogen bonds, such as those involving ⟩C═O, O−H, N−H groups, or aromatic nitrogen atoms, are very much involved in the aggregation properties of fluids, solids, and macromolecules, as noted above. Yet, hydrogen bonding to regions of excess aromatic π-electron density is also often highly significant. For example, it is the strongest interaction between "hydrophobic" molecules and hydrogen-bonding solvents such as water. Also, it may play a key role in the nucleation of water clusters and small droplets by large aromatic molecules or microscopic particles. One molecular-scale example of the relative significance of π-electron hydrogen bonding is found for the indole molecule under jet-cooled conditions, which exhibits two 1:1 complexes with water. Although no direct structural measurements have yet been published,[10] spectroscopic evidence, supported by structure calculations, strongly

[⊗] Abstract published in *Advance ACS Abstracts,* August 15, 1997.

S1089-5639(97)01674-5 CCC: $14.00

TABLE 1: Comparison of Computer Calculations with Rotational Coherence Data for Perylene[a]

	rotational constants		
calculation type	*A*	*B*	*C*
experiment[30]	620	335	218
CVFF[33]	628.2	335.3	218.6
CFF91[33]	623.6	337.0	219.4
AM1[43]	623.8	335.0	218.0
PM3[43]	625.7	337.5	219.3
SYBYL[43]	638.3	329.2	217.2
MNDO[43]	612.2	325.4	215.1

[a] Formally, one can assign the *B* and *C* constants for perylene separately, due to the presence of both C and J-type rotational coherence transients. The *A* constant is interpolated partly from structure calculations and also from "shape" information due to the rotational asymmetry.

suggests that one form involves hydrogen bonding to the ⟩N−H group, while the other is hydrogen bonded via the aromatic π-electron system.[11] The presence of these two species in comparable amounts suggests that the two types of interaction have comparable strength for indole.[12,13] Recent molecular mechanics calculations in this laboratory support these general conclusions.[14]

Much information has already been accumulated for water clusters nucleated by a single benzene molecule.[15−20] Extensive spectroscopic measurements have included infrared-optical and Raman-optical double-resonance studies aimed to probe the hydrogen bonds themselves, leading to the identification of several important types of water aggregates in clusters with benzene. Significantly, the above studies showed that small water clusters, either isolated or nucleated by a benzene molecule, have the same general types of structures.[21−23] The trimer, tetramer and pentamer have planar structures, or nearly so, while the hexamer exists as a three-dimensional "cage"-type structure. One reason for this similarity is that benzene can accommodate only a single hydrogen bond at this cluster size. Moreover, only one cluster of each type has been reported. Structure calculations of this system have also been applied using both molecular mechanics ("MMC")[24] and *ab initio* (i.e., MP2 and density functional) approaches.[21] On the other hand, it is possible that nucleation of water clusters by a larger molecule such as perylene, which can support two or more hydrogen bonds, could provide a means to stabilize other structural geometries of water aggregates. In the present study, we have expanded our own studies of perylene-based systems to include hydrogen-bonded clusters, focusing for the moment on the structures of 1:1 species.

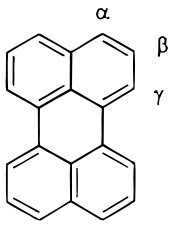

The $S_0 \leftrightarrow S_1$ transition of perylene is long-axis polarized, and the 0_0^0 transition has a high Franck−Condon factor. Also, while perylene itself is an asymmetric top, many complexes of this molecule are nearly prolate and are particularly suitable for rotational coherence studies.[4,5,25] The inertial properties of many complexes of perylene with non-hydrogen-bonding molecules have been determined in this way.[6,26−28] The site for optimum dispersion interaction is closest to the center of mass, as evidenced by the measured structures of complexes with small molecules and rare-gas atoms. On the other hand, the region of greatest π-electron density in an aromatic molecule such as perylene involves the α, β, and γ carbon atoms on the perimeter of the molecule, so that one may expect that molecules having strong hydrogen-bonded interactions could be drawn away from the center-of-mass site.

We have recently reported preliminary experiments, where rotational coherence spectroscopy was used to investigate the inertial properties of perylene 1:1 complexes with methanol and water.[29] The results were compared to predicted structures calculated by molecular mechanics routines. In the present study, we compare those cases with both straight-chain and branched alcohols, allowing a broader comparison of the results of structure calculations with experiment.

2. Experimental Procedures

Second-harmonic radiation from a Nd:YAG laser, mode-locked at 76 MHz, synchronously pumped a dye laser employing LDS 821 dye and IR-140 saturable absorber. The cavity-dumped output at 3.8 MHz was frequency-doubled in BBO to provide excitation wavelengths in the range 410−425 nm. Wavelength tuning involved a three-plate birefringent filter, yielding $\approx$5 cm^{-1} bandwidth after second-harmonic generation. The pulse durations were monitored via a spinning-mirror autocorrelator. The instrument-response time of the time-correlated single-photon counting apparatus, including the dye laser, detection monochromator, and 6-μm microchannel-plate detector, was 35−40 ps fwhm. For consistency in time calibration, we standardized the apparatus to the (J-type) recurrence time of perylene/octane, 3.42 ns,[27] which had in turn been cross-referenced against the original perylene RCS measurement by Felker et al.[30]

Spectral hole-burning experiments used a nitrogen laser to pump two grazing-incidence dye lasers,[31] each having a bandwidth $\approx$2 cm^{-1}. An optical delay of $\approx$60 ns separated the pump and probe pulses. Fluorescence excitation measurements used the attenuated output from one of these dye lasers.

Perylene crystals were heated (170−180 °C) in a small chamber mounted in the helium flow line immediately before the pulsed valve. The vapor of the complexing species was introduced from a side tube by bubbling helium through the liquid at room temperature.

Structure Calculations. The minimum-energy structures of the various 1:1 complexes were computed using several techniques, but primarily the constant valence force field (CVFF; molecular mechanics).[32,33] As we will show, the latter approach gave the most consistent results. The program, which is run through the Insight II graphical interface, uses an extensive library of molecules from a protein database (Biosym).[33] For reference, the CVFF-minimized structure of perylene closely reproduced the moments of inertia assigned by Felker and coworkers.[25] The results of this calculation, together with those from other procedures, are summarized in Table 1.

The minimization of a cluster structure proceeded from a user-defined set of relative initial coordinates for the component molecules. The procedure involved calculation of the total energy of the system, which was carried out with respect to intramolecular as well as intermolecular coordinates. For example, in addition to adjusting the relative molecular coordinates and orientations toward the minimum energy, the program adjusts internal coordinates such as torsional motion about single bonds and bond angles. As we will show, this permits simultaneous optimization of hydrogen-bonded and dispersion interactions, and in one case finds a different conformational isomer of an alcohol molecule. We also

TABLE 2: Intermolecular Interaction Parameters Used by CVFF[a]

atom code	atom type	A (cm^{-1})	B (cm^{-1})	q (au)
h	C−H hydrogen	2.487×10^6	1.150×10^4	0.1
c3	alkyl C−C and C−H carbon	6.263×10^8	1.849×10^5	−0.3 (terminal) −0.2 (primary) −0.07 (secondary) +0.03 (tertiary)
cp	aromatic sp^2 carbon	1.038×10^9	4.637×10^5	−0.1 (C−H) 0 (other)
c	alkyl C−O carbon	6.930×10^8	3.939×10^5	−0.17
oh	alcohol oxygen	9.546×10^7	1.745×10^5	−0.38
o*	water oxygen	2.201×10^8	2.188×10^5	−0.82
h*	alcohol hydrogen	0	0	+0.35
h*	water hydrogen	0	0	+0.42

[a] The nonbonded part of the potential energy function is: $E_{ij} = (A_{ij}/r_{ij}^{12}) - (B_{ij}/r_{ij}^{6}) + (q_i q_j/r_{ij})$, where $A_{ij} = (A_i A_j)^{1/2}$ and $B_{ij} = (B_i B_j)^{1/2}$. The notation h* applies to both the water and hydroxyl hydrogen atoms, for L-J purposes, whereas different parameters are used for oxygen in water and alcohols.

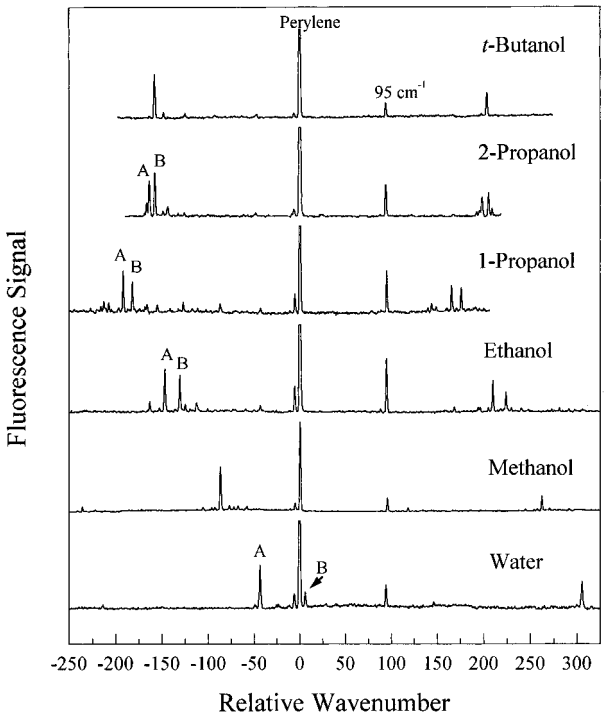

Figure 1. Sequence of fluorescence excitation spectra for complexes of perylene with water and alcohols. Species A and B are labeled so that the A species in each case has the greater red shift. All spectra are simple, showing little prominent vibronic structure. The labeled features to the left correspond to the electronic origin transitions of the complexes, while the features to the right, displaced ≈360 cm^{-1} from the origins, arise from the lowest a_g mode of S_1 perylene. The electronic origin transition of perylene occurs at 24 065 cm^{-1}.

employed the CFF91 force field, which includes an extra out-of-plane component to the energy calculation. Both the CVFF and CFF91 approaches gave structures for isolated perylene, which had rotational coherence signatures close to experiment.

For calculations involving the CVFF force field, the intermolecular interaction term has a simple Lennard-Jones 12-6 form, plus a correction for atom-center-based distributed point charges. All carbon atoms of perylene are treated the same (atom type "cp"; see Table 2), as are the carbon atoms in the alcohols (atom type c3), except for those attached to oxygen (c). Also, in CVFF, the charges on the perylene carbon atoms are simplified as compared with, for example, an AM1 calculation. Thus a charge of −0.1 is assigned to C−H carbons and +0.1 to the hydrogen atoms. Those aromatic carbon atoms not

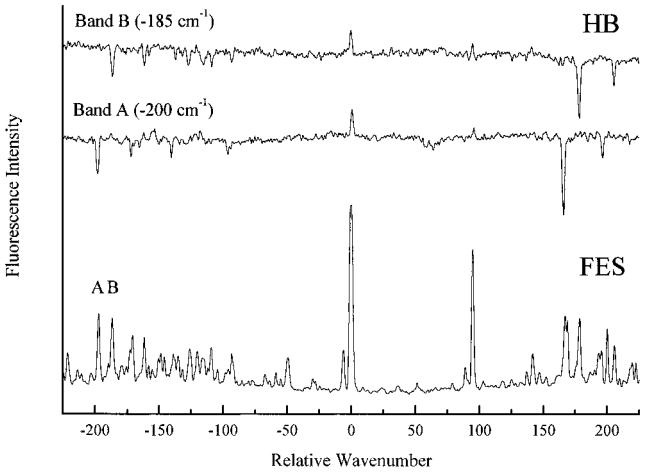

Figure 2. Sequence of spectra showing the resolution of the A and B species of perylene/1-propanol by electronic hole burning. Here, the low-frequency mode structure is exaggerated by saturation effects. The bottom trace (FES) and the hole-burning trace for species B were run at the same time. Trace A was added from a different run, after cross-calibration.

TABLE 3: Spectral Shifts of Different Hydrogen-Bonded Complexes of Perylene

complexing species	spectral shift (cm^{-1})
water (A)	−43
(B)	+5
methanol	−87
ethanol (A)	−147
(B)	−131
1-propanol (A)	−196
(B)	−186
2-propanol (A)	−164
(B)	−158
tert-butyl alcohol	−158

connected to hydrogen are assigned zero charge. Other parameters are given in Table 2. In the dual minimization procedure, the CVFF force field cycles twice through the intramolecular potential energy calculation for every calculation of the intermolecular interaction. To find the potential-energy minimum, the minimization procedure employs the Newton-Raphson method of steepest descent.

3. Results

a. Fluorescence Excitation/Hole Burning. Figure 1 shows a set of fluorescence excitation spectra for the different hydrogen-bonding species studied. They are aligned in the figure to use the perylene electronic origin transition as a reference. The features on the right arise from the lowest-energy a_g vibronic band of perylene, at 353 cm^{-1}. In the complexes, this frequency increased to ≈360 cm^{-1}. The perturbation for this in-plane mode is slightly greater than for nonpolar complexes, such as those involving *n*-alkanes. The spectra of the methanol and *tert*-butyl alcohol complexes indicate a unique type of structure in these two cases, whereas those involving water, ethanol, 1-propanol, and 2-propanol each display at least two electronic-origin transitions, labeled A and B. In each case, including the water complex,[29] hole-burning spectroscopy confirmed that A and B correspond to different ground-state species. For illustration, we show the result for the 1-propanol complex in Figure 2. The hole-burning data, recorded at much higher laser power than the excitation data in Figure 1, exaggerate the importance of weak, low-frequency modes. However, they also illustrate clearly the presence of two distinct excitation spectra. The spectral shifts for all species are listed in Table 3.

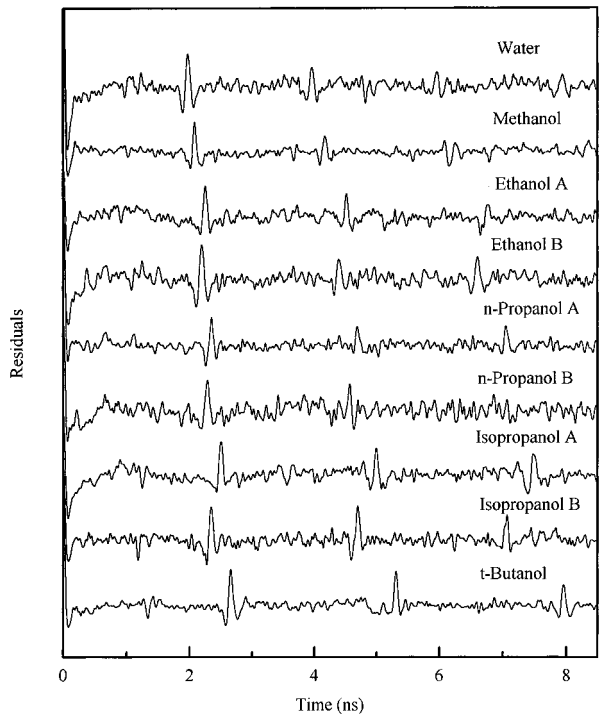

Figure 3. Summary figure of the rotational coherence traces obtained for hydrogen-bonded complexes of perylene.

TABLE 4: Rotational Coherence Properties of Perylene Hydrogen-Bonded Complexes

species excited	recurrence type	recurrence time (ns)	fluorescence decay time (ns)
water (A)	J	1.98	8.5
	C	1.21	
(B)			
methanol	J	2.10	8.8
	C	1.22	
ethanol (A)	J	2.26	8.0
(B)	J	2.21	9.6
	C	1.22	
1-propanol (A)	J	2.34	10.0
(B)	J	2.27	10.0
2-propanol (A)	J	2.48	9.9
	H	3.57	
(B)	J	2.34	9.5
tert-butyl alcohol	J	2.64	9.3
	H	5.04	

Apart from the above detail, the spectra of Figure 1 show only weak low-frequency mode structure, which could be attributed to Franck−Condon active intermolecular vibrations. This suggests that the structures of the complexes are similar in the ground and excited states. Consequently, a measurement of the excited state structure should approximate that of the ground state, at least to the precision needed for comparison with structure calculations.

b. Structure Calculations and Measurements. All species indicated in Figure 1 were also studied via rotational coherence spectroscopy, except for the water B species (for reasons of resolution).[29] Figure 3 and Table 4 summarize these results. Structure assignments involved the following procedures. Each component molecular structure was computed by molecular mechanics, using the CVFF force field. The complexes were then allowed to minimize, starting the system at different relative positions and orientations. This procedure identified more than one energy minimum in most cases, the notable exception being the methanol complex, which showed the same structure independently of the input parameters.

Whereas the CVFF force field kept the molecule planar, the CFF91 force field left perylene with a minor out-of-plane twist upon complexation. This still allowed a close fit to experiment. Since electronic excitation of perylene funnels electron density into the "peri"-bonds, inducing a more planar configuration, the presence of such a twist in the ground state would be expected to promote Franck−Condon activity in out-of-plane modes. One such appears at 95 cm^{-1} in the S_1 state of the bare molecule.[34] However, no prominent low-frequency mode structure was observed in the spectra of the complexes. Other procedures, such as the semiempirical AM1 and PM3 approaches, favored even larger out-of-plane distortion for complexes, and generally did not fit the experimental inertial data. The minimization procedure, which allowed adjustment of both intramolecular and intermolecular coordinates, commonly imposed minor structure changes on the alcohol molecules. One such change was a rotation about the C−O bond to optimize the hydrogen bond. Also, the calculations selected one structure of the 1-propanol complex, which involved a *gauche* isomer of the alcohol. Several examples of fits to experimental data are described in the following discussion. An important result of this procedure was that, in almost all cases, the initial coordinates computed from the molecular mechanics (CVFF) approach were sufficient to obtain a close fit to the experimental data.

For the structure corresponding to each minimum, we computed the inertial properties, which provided the starting point for fitting the rotational coherence traces. On the basis of an estimated structure, we used three rotational constants and an inertial axis rotation (usually close to zero) for the simulation procedure. However, one should note that in some cases, only J-type transients were confidently observed. For near-prolate tops, the spacing of these transients is $(B + C)^{-1}$, which provides little information about *A*, and the difference between *B* and *C* can only be interpolated indirectly. One should note, however, that the calculated structures define limits on *A* since this depends largely on the intermolecular separation perpendicular to the perylene plane. Since it is controlled by a fairly steep repulsive potential, this separation can be reliably estimated. Also, the value of the *C* constant depends on the radial distance of the complexing molecule from the axis perpendicular to the perylene plane.

Some cases showed other coherence transients, allowing a greater level of detail. For example, in several cases, which deviated significantly from the prolate symmetric top limit, the presence of C-type transients formally allowed separate measurement of the *B* and *C* rotational constants.[35] Also, for the *tert*-butyl alcohol complex and one conformer of the 2-propanol complex, the presence of hybrid transients signified partial perpendicular character for the transition, resulting from an inertial axis rotation. This formally allowed measurement of the *A* rotational constant plus the sum of the *B* and *C* constants.[25] However, these simple correlations are insufficient for structure assignment, since none of the species is a perfect prolate top. In asymmetric systems, deviations up to 50 ps between the J-type recurrence time and $(B + C)^{-1}$ are common, whereas structural fits often require a precision <20 ps. Therefore, direct simulations of the rotational coherence data were carried out in each case using a procedure distributed by Felker and coworkers.[25,36−38] This involves calculating the rotational eigenstates for a rigid-rotor asymmetric top model and subsequent calculation of the Fourier transform of the appropriate beat-frequency spectrum for two-photon rotational coherences. (i.e., one photon in excitation and one in spontaneous emission). The simulations not only locate the recurrence transients but also provide valuable shape information, which can define a

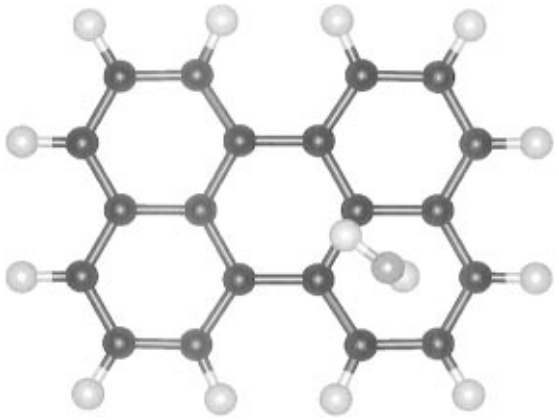

Figure 4. Calculated (CVFF) structure of the water complex of perylene.

TABLE 5: Calculated Displacements of Complexing Molecules, Referenced to the Center of Mass of Perylene[a]

complex	displacements (Å)			out-of-plane displacement of oxygen atom (Å)
	x	*y*	*z*	
water	1.87 (0.3)	0.89 (−0.1)	3.22 (0)	3.27
methanol	1.27 (0.3)	0.53 (−0.1)	3.33 (0)	3.14
ethanol (A)	1.33 (−0.1)	0.19 (−0.4)	3.54 (0)	3.16
ethanol (B)	1.20 (0)	0.39 (0)	3.52 (0)	3.16
n-propanol (A)	0.88 (0)	0.18 (0)	3.61 (0)	3.24
n-propanol (B)	0.42 (−0.1)	1.44 (0.2)	3.61 (0.1)	3.12
2-propanol (A)	1.36 (0.4)	0.35 (−0.4)	3.68 (0.2)	3.16
2-propanol (B)	1.05 (0)	0.94 (0)	3.67 (0.1)	3.16
tert-butyl alcohol	1.45 (0)	0.51 (0)	3.99 (0.1)	3.13

[a] The *x*, *y*, *z* coordinates refer to the calculated displacements by CVFF. The numbers in parentheses represent the further displacements need to match experimental data. To fit the numbers for the A form of 2-propanol, a 10° rotation about the *x* axis was required, along with the above stated displacements. For *tert*-butyl alcohol, a 5° rotation was used.

structure.[25] For example, in the present study, we observed interferences between J-type and C-type recurrence transients. This happens after several recurrences of both since, in the prolate top range where C-type transients are observed, the *B*/*C* ratio varies in the range 1.2−1.5. As has been noted elsewhere, C-type transients vary in shape, amplitude and polarity, so that in a given sequence some transients may not be observed.[30] One may note that an advantage of using photon-counting analysis is that the rotational coherence transients can be tracked in the same experiment usually through several recurrences. The technique is limited by the instrument response function (35−40 ps) and by the photon-counting rate and system long-term stability.

Water. The results for water and methanol complexation of perylene were reported in a preliminary publication.[29] Minimization of the interaction energy for the perylene/water 1:1 complex gave the structure shown in Figure 4. This has the water molecule displaced from the center of mass of the perylene molecule, so that it is hydrogen bonded to one of the outer rings. The center-of-mass coordinates are listed in Table 5. A second minimum was also calculated, in which the water molecule is bonded symmetrically to the center of the perylene molecule. Although we are not sure whether this centrally bonded form is observable, our experimental data convincingly show that band A in the excitation spectrum of Figure 1 is due to a structure such as in Figure 4. This structure gave rise to a set of rotational constants $A = 513$, $B = 291$, $C = 211$ MHz. Data for all the species studied, with their calculated binding energies, are listed in Table 6.

The experimental and simulated rotational coherence traces for the water (A) species and the single methanol complex, which were reported in the preliminary study,[29] are reproduced in Figure 5. The model for the simulation assumed a parallel transition. Here, the presence of C-type transients played an important role in the structure assignment. For example, without knowledge of the *C* rotational constant, a water molecule could be placed directly above the perylene center of mass at relative center of mass coordinates (0, 0, 3.5 Å) and still yield the experimentally determined value of the J-type recurrences. However, the departure of the C-transient spacing from that of bare perylene reflects mass displacement from the out-of-plane symmetry axis of the perylene molecule. Thus, perylene has C-transient spacing of ≈1147 ps, and a water molecule directly over the central axis would have a C-transient spacing of ≈1148 ps—essentially the same, having only hydrogen atoms displaced from the axis. Instead, the experimentally measured value of 1210 ± 10 ps, based on measurements of the first and fourth C-type recurrences, confirms a significant displacement from the center of mass.

The "513" notation in Figure 5 corresponds to the coordinates taken directly from the CVFF-minimized structure. Most of the features in the experimental trace were reproduced well. The "491" trace results from a best fit to the shape of the J-transient near 6 ns, which is attributed to an interference with a C transient, by reducing the value of *A*. This variation represents our uncertainty in assigning the *A* constant. Note that the values of the *B* and *C* constants, however, can be assigned with little error, because of the presence of both J-type and C-type transients. The experimentally derived constants, based on the best fit, were $A = 491$, $B = 288$, $C = 207$ MHz. These are also listed in Table 6.

We have not yet assigned the B band of the water complex, due to the low spectral resolution of the rotational coherence apparatus (i.e., 5 cm^{-1}, as compared with 6 cm^{-1} shift from the bare-molecule 0_0^0 band). This may represent a structure having the water bound over the center of mass of the perylene molecule, but it could also be due to a second nuclear spin isomer such as reported by Zwier et al. for the benzene case.[18] We plan to investigate this band further, via a higher-resolution rotational coherence experiment.

Methanol. An important aspect of the calculation is shown for complexes involving larger molecules. Thus, while the displacements of the centers of mass can be estimated from the experimental data, another reference tool is needed to determine the molecular orientation. The clear prediction from the CVFF calculations is the single structure shown in Figure 6, in which the methanol molecule is hydrogen bonded to the same location as the water complex. Moreover, the structure shown was calculated to be more stable than a centrally-hydrogen-bonded structure corresponding to 180° rotation of the methanol molecule, by ≈130 cm^{-1}. This difference was almost entirely due to the electrostatic contribution. The structure shown in Figure 6 gave, to within 0.3 Å, a set of rotational constants from which the experimental results could be simulated.

Consistent with the CVFF predictions, methanol complexation revealed only a single species, having a red shift of 87 cm^{-1} (see Figure 1). The rotational coherence data (see Figure 5) again show the presence of C transients, which provides a direct measure of the *C* rotational constant. As in the water case, this provides the means to assign the displacement of the complexing molecule from the center of mass of the perylene host species. Thus, a methanol molecule directly over the center of mass would give a C-type transient spacing of ≈1157 ps, as compared with the experimental value of ≈1220 ps. The rotational

TABLE 6: Rotational Constants and Calculated Binding Energies of Perylene Hydrogen-Bonded Complexes

	calculated (CVFF) (MHz)			calculated binding energy (cm^{-1})			experimental fit (MHz)		
	A	*B*	*C*	Coulomb (%)	L-J	total	*A*	*B*	*C*
water (outer)	513	291	211	−847 (60)	−556	−1402	491	**288**	**207**
methanol	449	269	211	−668 (30)	−1553	−2221	449	**267**	**205**
ethanol (A)	393	239	204	−609 (23)	−2078	−2686	393	*239*	*200*
ethanol (B)	382	245	206	−595 (23)	−2053	−2648	382	**244**	**205**
1-propanol (A)	344	223	201	−567 (18)	−2651	−3218	344	**223**	**201**
1-propanol (B)	311	244	190	−483 (16)	−2466	−2949	311	**239**	**190**
2-propanol (A)	344	219	197	−626 (20)	−2505	−3131	**338**	**205**	**194**
2-propanol (B)	330	230	194	−567 (19)	−2456	−3022	333	*230*	*193*
tert-butyl alcohol	296	197	183	−644 (18)	−2840	−3484	**289**	*195*	*181*

[a] Experimental numbers in **boldface** are individually determined by experiment, those in *italics* are determined as a pair, and the others are quoted as they fit the CVFF calculation. The exception is the water complex, which is discussed in Figure 5.

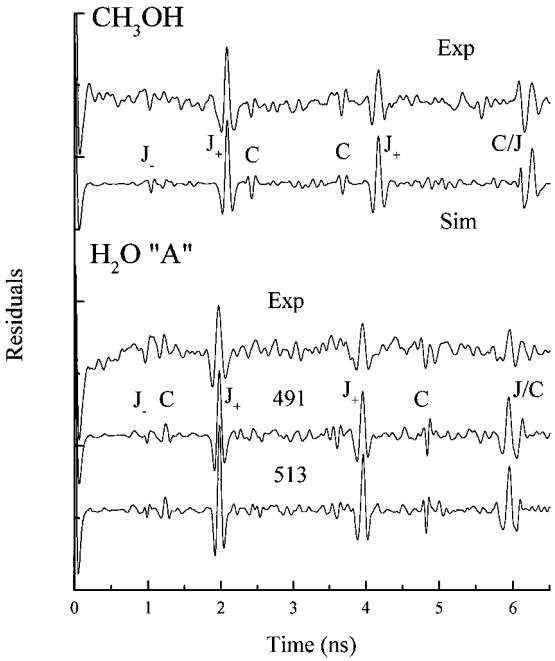

Figure 5. Comparison of rotational coherence traces with simulations for the water and methanol complexes of perylene. (Lower) The notations 491 and 513 indicate different choices of the *A* constant for simulation of the water complex. The latter matches the CVFF simulation, while the former represents an attempt to match the shape of the interference near 6 ns. (Upper) In addition to the J-types, an interference feature near 6 ns and two C-type features are matched.

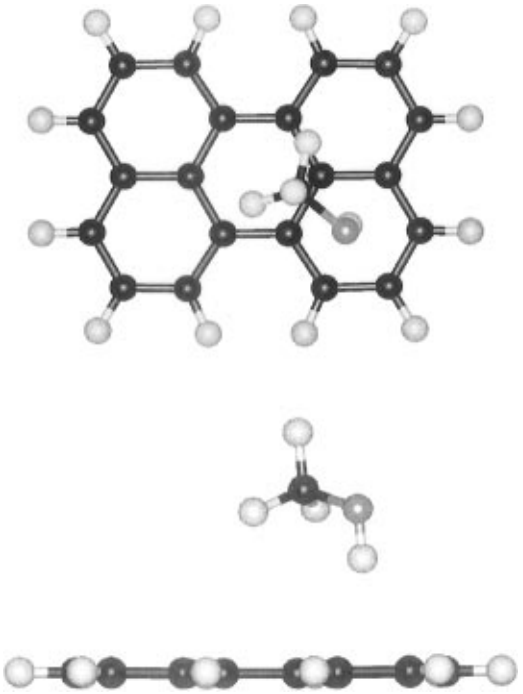

Figure 6. Two views of the calculated structure of the methanol complex of perylene.

constants used to simulate the experimental data were $A = 449$, $B = 267$, $C = 205$ MHz, again assuming a parallel transition. As Table 5 shows, a small displacement was needed from the CVFF minimum structure to match these constants.

Ethanol. The fluorescence-excitation and hole-burning spectra for ethanol/perylene confirm the existence of two distinct species labeled A and B, red-shifted by 147 and 131 cm^{-1}. The ethanol case is slightly unusual, compared with the other cases in the current study, since the fluorescence decay times of the A and B species are significantly different (see Table 4). However, such lifetime differences are common in small-molecule complexes of perylene and even for perylene itself following excitation via different vibronic bands. For example, the fluorescence decay times of the two conformers of 2:1 complexes of methane with perylene also differ significantly (i.e., 8.4 ns for (2|0) and 9.2 ns for (1|1)).[39] This may be due to accidental differences in singlet−triplet coupling.

The CVFF calculation for ethanol/perylene predicts two low-energy structures, as shown in Figure 7. They are predicted to have comparable stabilization energies as follows: $E_{(A)} = -2686$; $E_{(B)} = -2648$ cm^{-1}. These two structures have in common a hydrogen bond to an outer ring of perylene, the *z*-axis distance between centers of mass is ≈3.53 Å, and the oxygen out-of-plane distance is ≈3.16 Å. They differ in the rotation of the inertial axis of the ethanol molecule with respect to the perylene long axis: (A ≈30°, B ≈90°).

In order to simulate the experimental trace for band A, the rotational constants $A = 393$, $B = 239$, $C = 200$ MHz were used. It has been our experience, where different structural conformers are present for molecular complexes of perylene, that those complexing molecules having the greater red shifts tend to have their long axes (i.e., axis of greatest polarizability) aligned parallel to the perylene long axis (i.e., the $S_0 \leftrightarrow S_1$ transition moment). The A species for ethanol has its axis ≈30° from the perylene long axis, as the structure in Figure 7 shows. Such species also tend to exhibit longer J-type recurrence times.

In the rotational coherence trace for band B of the ethanol complex, we observed J-type recurrences at 2.21 ns and a C-type recurrence time of 1.22 ns. Figure 8 shows a section of the rotational coherence trace for this species, focusing on the first J-type transient and the second C-type. In the present case of the B structure for ethanol/perylene we found excellent agreement between the experimental observations and the predicted second structure from molecular mechanics calculations, which is shown in Figure 7. Note that this structure has the ethanol long axis aligned close to the short axis of perylene.

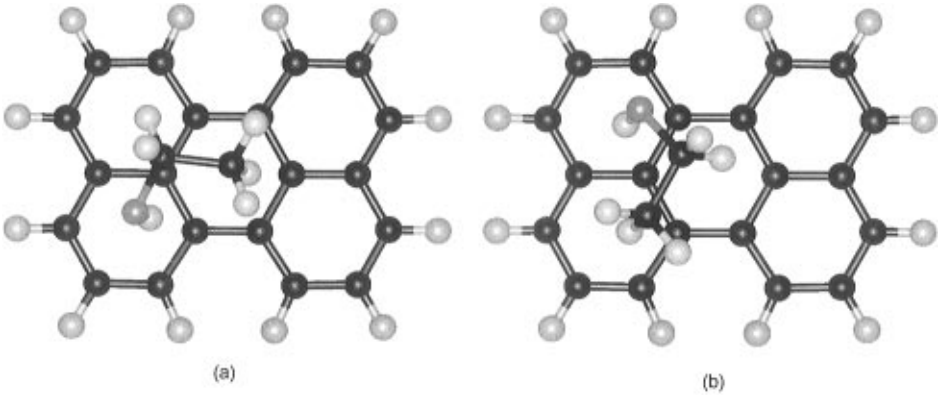

Figure 7. Calculated structures of the two conformers of the ethanol complex (a) A, (b) B.

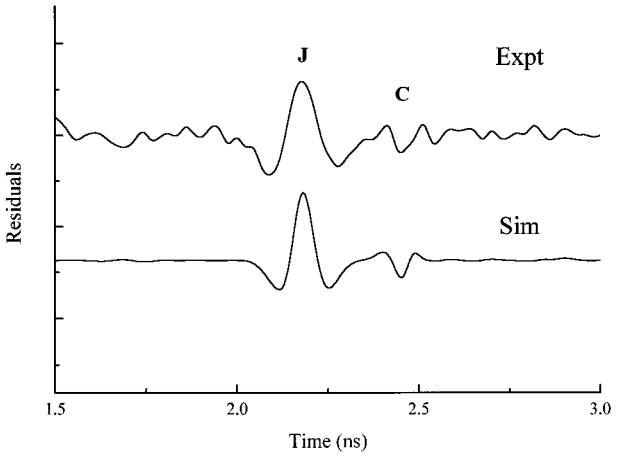

Figure 8. Detail from the rotational coherence trace for ethanol, showing a residual C-type transient.

1-Propanol. We did not accumulate the 1-propanol rotational coherence data for as long as some of the other species, limiting the interpretation of the data. Nonetheless, the data presented in Figure 3 show J-type progressions similar to those for the ethanol case. Excitation via band A gives a recurrence time ($\tau_J \approx 2.34$ ns), which is 70 ps longer than that of band B ($\tau_J \approx 2.27$ ns). Like the ethanol case, for the species exhibiting the greater red shift and the longer J-type recurrence time, we look for a structure having a long-axis orientation. The CVFF structure suggested for the A species is close to this, yielding rotational constants $A = 344$, $B = 223$, $C = 201$ MHz, which places the 1-propanol long-axis at 30° to the long axis of perylene. Moreover, the CVFF structure gave a simulated rotational coherence trace exactly matching the experimental result. As can be seen from Figure 9, the structure calculation again places the hydrogen bond close to the center of an outer ring.

Band B appears to break the trend of the other structures shown here. The spacing of the J-type transients, which is ≈70 ps less than that for the A band, presents some difficulty for the molecular mechanics calculations. If we constrain the 1-propanol structure to remain in the all-*trans* position, energy minimization tends to pull the end methyl group and terminal −OH group above diagonal rings of the perylene to give the band A structure. We could fit the experimentally observed recurrence time, by simply aligning the alcohol long axis at 90° to the perylene long axis. However, this did not correspond to a computed energy minimum and must therefore be suspect.

On the other hand, if we did not constrain the alcohol structure, the minimization frequently arrived at the other structure shown in Figure 9. This involves a *gauche* form of the alcohol and gives with little adjustment the experimentally measured recurrence time of 2.27 ns.

In conclusion, the 1-propanol molecule is an important case for future study, as it represents a situation where the optimum dispersion interaction should destabilize the hydrogen bond in the position for the other alcohol complexes. This creates an increased possibility for twisting the complexing molecule. The situation should be more evident for longer-chain alcohols. Despite the excellent agreement between calculation and the existing experimental data, it is clear that more precise rotational coherence data are required, in order to support the increasingly less certain calculations.

2-Propanol. The molecule 2-propanol provides an interesting test case for how the complex structure will begin to respond to a branched alcohol. In principle, one may suspect that the hydrogen-bonded part of the potential should become more prominent, as the structure of the alcohol forces one of the carbon atoms away from the aromatic surface. Figure 1 shows that the loss of dispersion interaction is evident from the blue shift of the complexation resonances, as compared with 1-propanol. Moreover, the tetrahedral distribution of R-groups around the central carbon atom naturally implies a trigonal coordination with respect to the aromatic surface. In reference to earlier work, we showed that the trigonal coordination geometry caused the cyclopropane complex of perylene to have an off-center geometry in the absence of a hydrogen bond, also verified by rotational coherence spectroscopy.[26]

The 2-propanol complex exhibits two closely spaced bands at red shifts of 158 and 164 cm^{-1}. Again, hole-burning data reveal these to be distinct species. The spacing of 6 cm^{-1} is the smallest for the sequence of alcohols in the present study, showing that the binding energy is influenced to about the same degree by electronic excitation of the perylene molecule. On the other hand, the J-type transients for these two species have the greatest difference, at 140 ps (i.e., ≈6%), which is twice that observed for the 1-propanol case. This confirms a significant difference in the mass distribution between the two species.

The rotational coherence trace for band A shows four prominent J-type recurrences with spacing $\tau_J \approx 2.48$ ns, plus a weak negative hybrid transient at ≈3.5 ns (see Figure 10). Also, although they are weak in the experimental trace, two C transients appear in the simulation near 2.8 ns (2nd) and 6.9 ns (5th), which appear to match features in the experimental trace. Despite noise in that trace, this appears to confirm our assignment for the *C* constant. The presence of the hybrid transient indicates that the principal inertial axis is tilted with respect to the $S_0 \leftrightarrow S_1$ transition moment. These transients reflect the partial perpendicular character of the transition, and the presence of beat frequencies resulting from consecutive

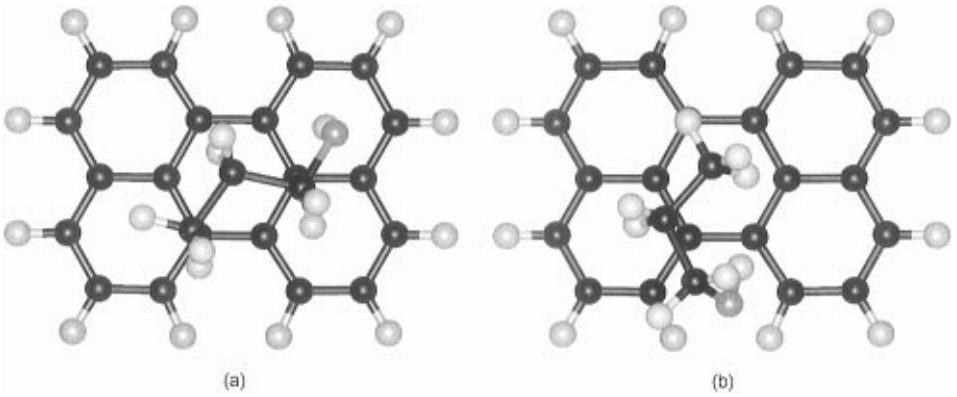

Figure 9. Calculated structures of the two conformers of the 1-propanol complex (a) A, (b) B. This postulated B form contains a gauche form of the alcohol molecule.

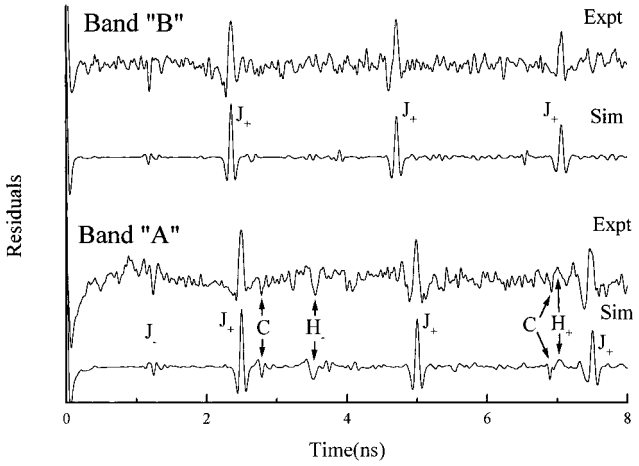

Figure 10. Two rotational coherence traces for the 2-propanol complex, each compared against the simulation. Whereas band B gives no identifiable extra features, the simulation of band A, based on the calculated structures, suggested both C-type and weak hybrid features.

transitions involving an overall change $\Delta K = \pm 1$.[25] Structure calculations for the A species suggest a tilt of ≈14°.

The CVFF calculation predicts two potential-energy minima. The one corresponding to the longer recurrence time of $\tau_J \approx$ 2.48 ns has the −OH group and one methyl group in two outer rings and the remaining methyl in the center ring. The calculated structure for the A species of 2-propanol/perylene needed a small displacement to match the experimental results (See Table 5). These corrections were small enough that the site of attachment could be definitively identified. The proposed structure is given in Figure 11.

The second conformer, band B, has $\tau_J \approx$ 2.34 ns and the experimental trace in Figure 10 shows that the value of $B + C$ is ≈6% different from that of the A species. Moreover, the simulation did not suggest any prominent C-type or hybrid transients. The former suggests a higher rotational symmetry and the latter that the 2-propanol molecule is closer to the center of mass, such that the inertial axis rotation is small. This observation is also consistent with the reduced spacing of the J-type transients. The structure suggested by the molecular mechanics minimization, shown in Figure 11b, required ≈0.1 Å adjustment to match the observed J-type transients.

tert-Butyl Alcohol. The fluorescence excitation spectrum shows a single form of the *tert*-butyl alcohol complex. Also, despite the addition of a methyl group, there is no further red shift from the 2-propanol case. However, consistent with the increased mass, the spacing of the J-type transients has increased to 2.64 ns. Moreover, like the A form of 2-propanol, the experimental data also reveal hybrid transients. Figure 12 shows the first negative lobe near 5 ns and the first positive lobe near 10 ns. As with the 2-propanol case, the presence of hybrid transients reveals that the inertial axis has rotated from the direction of the transition moment, assumed still coincident with the perylene long axis. This in turn confirms that the center of mass of the *tert*-butyl alcohol molecule is displaced from the central position on the perylene molecule, as with the other alcohol complexes.

The structure of the *tert*-butyl alcohol complex of perylene was very well predicted by the CVFF model (See Table 5). The simulation helps to point out the broad component near 5.0 ns, occurring before the second positive J-type at 5.28 ns. In this case, we calculate that the principal inertial axis of the complex is tilted from the transition moment by ≈23°.

As can be seen from the structure shown in Figure 13, the *tert*-butyl alcohol complex involves a structure similar to the 2-propanol band A. On the other hand, it is significant that molecular mechanics techniques also predicted a second structure for the *tert*-butyl alcohol complex similar to the B structure for 2-propanol. However, our experiment yielded only a single species.

4. Discussion

The Molecular Mechanics Approach. The molecular mechanics approach provides a computationally efficient means to calculate the structures of isolated molecules and clusters of molecules, without directly using quantum mechanics.[32,40,41] The application of such techniques to compare the minimum energy structures of van der Waals complexes with structural data has been recently reported.[8,29,42] However, it is necessary to explain the reasoning for using this approach in the specific systems we are studying, since the hydrogen bond has traditionally been one of the more difficult cases to model. Molecular mechanics is a relatively simple computational technique, based on "classical" ideas of bonding and using simplistic nonbonded interactions, whereas there exist numerous more precise approaches to calculate such interaction potentials. Indeed many studies involving *ab initio* MP2 calculations have been performed on the interaction of water molecules with different classes of aromatic molecules. However, the largest of the complexing parent molecules studied in this way have been on the order of the size of benzene.[21] Perylene and other polycyclic aromatic molecules having importance in solvation problems are substantially larger, and the scaling factor of $\approx N^4$ for *ab initio* techniques make the "exact" approaches impractical, or costly. Semiempirical techniques such as AM1 or PM3 help to alleviate some of the computational intensity (N^2 dependence) and in fact play a valuable role in predicting charge distributions, transition moments, and vibrational modes of covalently bonded

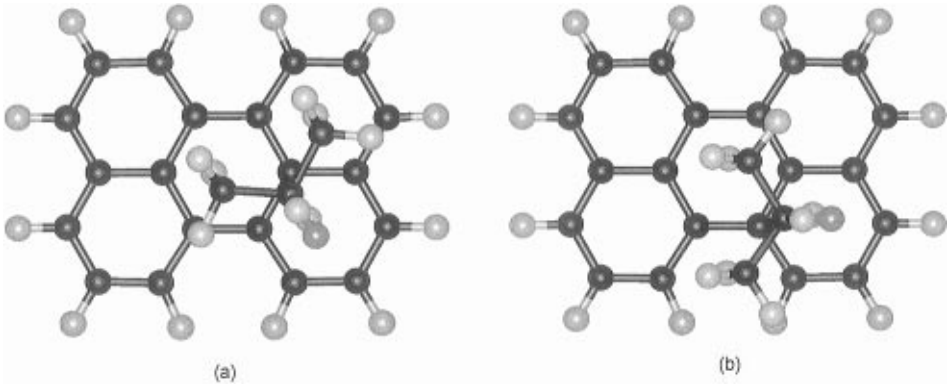

Figure 11. Calculated structures for the 2-propanol complex, showing both types to be hydrogen-bonded to the outer ring. The A species, having the greater J-spacing, has both methyl groups directly over aromatic rings. The B species is similarly hydrogen bonded, but lies in a more transverse position.

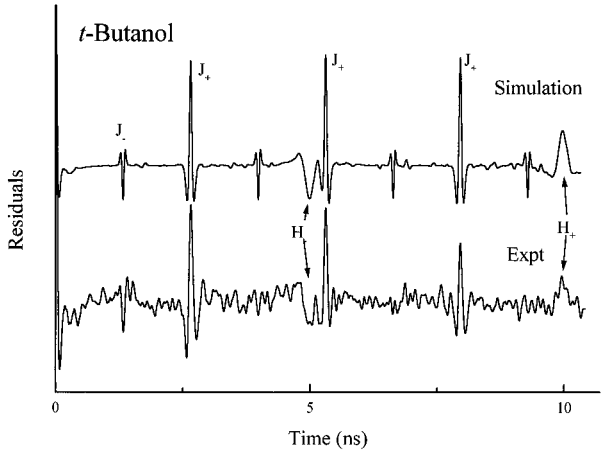

Figure 12. Comparison of the trace for *tert*-butyl alcohol/perylene with a simulation. Several strong J-type transients are observed, plus a prominent pair of hybrid transients.

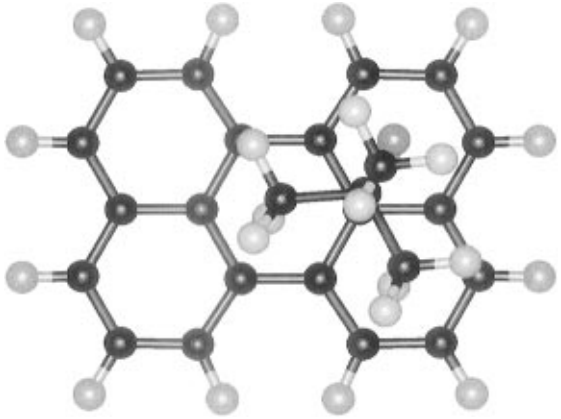

Figure 13. Calculated structure of *tert*-butyl alcohol/perylene. This structure is basically the same as the A-type structure of the 2-propanol complex, having the alcohol hydrogen bonded to an outer ring.

molecules. However, these techniques rely on empirical data, little of which is available for intermolecular interactions, beyond Lennard-Jones parameters. The combination of improper, or incomplete parameterization, along with the neglect of diatomic overlap makes them highly unreliable for predicting the structures of molecular aggregates.[43] This is consistent with our findings.

Instead, we have made use of the molecular mechanics force fields CVFF and CFF91, coupled to the Biosym database, and both graphed and minimized via the Insight II platform.[33] The difference in the intermolecular part of the potential lies in the Lennard-Jones repulsive term, which, in CFF91, varies with $1/r^9$ and in CVFF varies with $1/r^{12}$. For the perylene−alcohol series, the two force fields gave similar results, although CFF91 tends to distort the aromatic molecule from a planar geometry. This arises from an extra out-of-plane distortion term, present in CFF91.

TABLE 7: Comparison of Results from Other Structure Calculations

complexing species	force field	*A*	*B*	*C*	*B* + *C*
water	AMBER	531	308	220	528
	OPLS	518	299	212	511
	CFF91	513	295	211	506
	CVFF	513	291	211	502
	exptl	**491**	**288**	**207**	**495**
methanol	AMBER	455	272	214	486
	OPLS	451	274	212	486
	CFF91	447	269	207	476
	CVFF	449	269	211	480
	exptl	**449**	**267**	**205**	**472**
2-propanol (A)	AMBER	353	225	195	420
	OPLS	347	222	201	423
	CFF91	342	221	193	414
	CVFF	344	219	197	416
	exptl	**338**	**205**	**194**	**399**
tert-butyl alcohol	AMBER	285	209	198	407
	OPLS	298	194	191	385
	CFF91	294	201	178	379
	CVFF	296	197	183	380
	exptl	**289**	**195**	**181**	**376**

All complexes in this study, except for one species involving 1-propanol, indicated hydrogen-bond formation to an outer ring of the perylene moiety. In the water case, as Table 6 shows, the binding energy is primarily electrostatic (60%), whereas for the larger alcohols, this fraction is about 20%. A successful structural model must be able to balance the two types of contribution, especially considering the need to extend studies to larger clusters.

We compare in Table 7 the predictions of different molecular mechanics force fields, including CVFF, CFF91, AMBER,[44] and OPLS,[44] with experimental results. In all cases, we used a dual minimization approach, where the intramolecular and intermolecular interactions were simultaneously optimized, and no external constraints were imposed. It is clear from the examples given that CVFF and CFF91 yielded consistently the closest approximation to the experimental result, on the basis of the numerical values of the rotational constants. Since we saw J-type transients in all cases, the value of $(B + C)$ is a useful comparison tool. One should note that a variation of >1% in this quantity is considered to be significant, as this

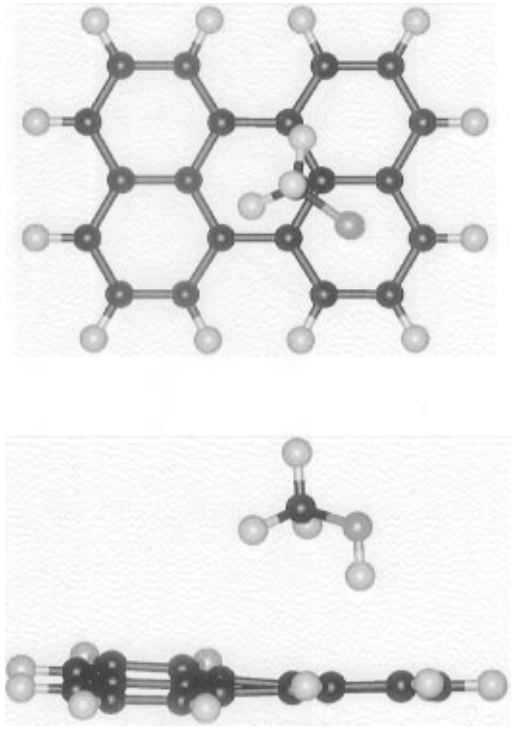

Figure 14. Two views of the methanol/perylene structure predicted by CFF91, showing the calculated twist of the aromatic molecule. Despite the difference from the structure shown in Figure 6, the rotational coherence predictions were basically the same.

represents the precision of our absolute time calibration. The experimental measurements were usually fit over a range >8 ns.

First, like CFF91, the AMBER and OPLS force fields tended to twist the aromatic ring. There is some evidence to support such a deformation in the isolated molecule, considering the Franck−Condon activity of the (overtone) band at 95 cm^{-1}.[34] However, the extent of deformation when complexes were formed appeared exaggerated under these simulations. As an example, Figure 14 shows the result obtained from CFF91, which obtains a twisted structure for the perylene molecule in the methanol complex. Although such a twisted structure seems counterintuitive, considering the weak intermolecular mode Franck−Condon activity, the rotational constants from the CFF91 calculations are still close to experiment (See Table 7). AMBER and OPLS tended on average to give poorer agreement with experiment. Particularly conspicuous is the failure of AMBER to model the water complex, giving a center-of-mass bound structure.

On the other hand, all force fields used gave better agreement with experiment when the perylene molecule was held in a rigid, planar structure, using the model optimized by CVFF. For example, by using AMBER in a mode where only the complexing molecule was allowed to minimize (i.e., single minimization), we were able to calculate rotational constants in good agreement with experiment. However, despite improved agreement for the correct rotational constants, neither the AMBER nor OPLS force field properly represented the hydrogen bond for either the water or the methanol complex. While AMBER did predict the correct structure for the *tert*-butyl alcohol complex (with rotational constants closely matching experimental values) for the single minimization technique, it also predicted only one conformer for 2-propanol, instead of the two observed forms.

Several general trends can be predicted from the use of the above force fields. First, all but CVFF allow for a significant ring distortion in the perylene molecule. In general, however, the results for the calculated and experimentally measured structures show good qualitative agreement. This is especially true for the CVFF, CFF91 and to a lesser extent AMBER and OPLS, where the significant deviations are due to twisting of the perylene molecule. We note that the different force fields use various Lennard-Jones potential forms (for example, CVFF uses 6-12, CFF91 6-9, and AMBER 6-12 nonbonded plus a 10-12 hydrogen bond term) and yet yield similar structures. Successful structure predictions confirm that each of these force fields achieves an appropriate balance between Lennard-Jones terms and the predicted electrostatic contribution to the interaction potential. In all but one case, that of the postulated gauche *n*-propanol conformer, the hydrogen bond is seen to form to the outer rings of the perylene molecule. This is consistent with optimizing the Coulomb interaction between the positively charged hydrogen and the negatively charged carbons on the outer ring.

Another point to note is that, usually, excited-state structures are more difficult to model since molecular mechanics techniques are parametrized for the electronic ground states. Strictly, rotational coherence measurements should be made for ground-state species via the TRFD (time-resolved fluorescence depletion) pump−probe type of technique.[25,45] However, the vibronic spectra of large aromatic hydrocarbons such as perylene suggest small structural changes between the ground and excited states. This has to some extent been verified by the work of Felker and co-workers.[4,5] Also, Figure 1 of this paper shows only weak vibronic structure attributable to intermolecular motion. Therefore, we expect small errors to be incurred in this study when comparing excited-state measurements with ground-state calculations. This is, however, not always a valid assumption, even for a single molecule, as work on *p*-cyclohexylaniline has shown.[46,47]

The molecular mechanics approach is particularly helpful in predicting multiple conformers, as in the cases of ethanol, 2-propanol, and *n*-propanol. For example, for ethanol, the CVFF and CFF91 calculations both predict two structures with similar binding energies. We note that the fluorescence excitation spectrum suggests that species A is in slight excess. This would be consistent with the increased binding energy for the CVFF predicted structures. However, the measured binding energies should not be used alone as a criterion for complex formation, since cluster formation dynamics must be considered. Also, the data we have obtained for the minimum energy conformer of the *n*-propanol complex suggests the presence of a different isomer of the complexing molecule. This is supported by the reported existence of the *gauche* form of *n*-propanol under supersonic jet conditions.[48]

As a final example, we recall that although the molecular mechanics routines predict a similar outcome for 2-propanol and *tert*-butyl alcohol complexation with perylene, the spectroscopic data clearly point out two conformers for 2-propanol, but only one for *tert*-butyl alcohol. We note that the structure calculations predict that the two species differ in stability by ≈100 cm^{-1} in both cases. We have identified all three observed structures but at this point do not have an explanation for why a B conformer of the *tert*-butyl alcohol complex is absent. Such an occurrence may be due to dynamical considerations, involving facile interconversion during complex formation. However, this explanation remains speculative at this point.

5. Conclusion

This study has brought together experimental techniques to measure the inertial properties of simple clusters with structure

calculations. This provides a powerful tool for assignment of structures of the test species, since neither approach alone is definitive. For example, the combination of rotational constants assignable from experiment is not sufficient to define a particular structure. Also, rotational coherence techniques alone cannot locate hydrogen atoms or distinguish spatial configurations of complexing molecules differing by end-over-end rotation.

In combination, the experiments and molecular mechanics calculations have shown that all species examined have in common a hydrogen bond to a region close to the perimeter of the aromatic molecule. It is noteworthy that several alcohol complexes exhibit dual structures under supersonic cooling conditions and that these structures can also be predicted via molecular mechanics procedures.

Future work will investigate the formation of larger hydrogen-bonded and other polar clusters involving perylene, as this species provides an excellent platform to investigate large clusters. It will be interesting to compare the types of water clusters formed on perylene with published work for water clusters either alone or nucleated by a benzene molecule. An important difference between the cases is that water clusters have been found to be bonded to benzene via a single π-hydrogen bond, whereas perylene offers the chance for at least double hydrogen bonding. This is quite favorable, since the present work has shown that the preferred hydrogen-bonding site for water on perylene is displaced from the center, creating opportunities for simultaneous optimization at more than one site.

Acknowledgment. This work was supported by the National Science Foundation (CHE-95-21362).

References and Notes

(1) Doxtader, M. M.; Mangle, E. A.; Bhattacharya, A. K.; Cohen, S. M.; Topp, M. R. *Chem. Phys.* **1986**, *101*, 413.
(2) Price, S. L.; Stone, A. J. *J. Chem. Phys.* **1987**, *86*, 2859.
(3) Castella, M.; Millié, P.; Piuzzi, F.; Caillet, J.; Langlet, J.; Claverie, P.; Tramer, A. *J. Phys. Chem*. **1989**, *93*, 3941.
(4) Ohline, S. M.; Joireman, P. W.; Connell, L. L.; Felker, P. M. *Chem. Phys. Lett.* **1992**, *191*, 362.
(5) Joireman, P. W.; Connell, L. L.; Ohline, S. M.; Felker, P. M. *Chem. Phys. Lett.* **1991**, *182*, 385.
(6) Troxler, T.; Stratton, J. R.; Smith, P. G.; Topp, M. R. *Chem. Phys. Lett.* **1994**, *222*, 250.
(7) Smith, P. G.; Topp, M. R. *Chem. Phys. Lett.* **1994**, *229*, 21.
(8) Pryor, B. A.; Andrews, P. M.; Palmer, P. M.; Topp, M. R. *Chem. Phys. Lett.* **1997**, *267*, 531.
(9) Pryor, B. A.; Andrews, P. M.; Palmer, P. M.; Berger, M. B.; Topp, M. R. Submitted for publication.
(10) Pratt, D. W. Private communication.
(11) Tubergen, M. J.; Levy, D. H. *J. Phys. Chem.* **1991**, *95*, 2175.
(12) Muiño, P. L.; Callis, P. R. *J. Chem. Phys.* **1994**, *100*, 4093.
(13) Muiño, P. L.; Callis, P. R. *Chem. Phys. Lett.* **1994**, *222*, 156.
(14) Andrews, P. M.; Berger, M. B.; Topp, M. R. Unpublished work, 1997.
(15) Gotch, A. J.; Garrett, A. W.; Severance, D. L.; Zwier, T. S. *Chem. Phys. Lett.* **1991**, *178*, 121.
(16) Augspurger, J. D.; Dykstra, C. E.; Zwier, T. S. *J. Phys. Chem.* **1992**, *96*, 7252.
(17) Kim, K.; Jordan, K. D.; Zwier, T. S. *J. Am. Chem. Soc.* **1994**, *116*, 11568.
(18) Pribble, R. N.; Zwier, T. S. *Faraday Discuss. Chem. Soc.* **1994**, *97*, 229.
(19) Pribble, R. N.; Zwier, T. S. *Science* **1994**, *265*, 75.
(20) Maxton, P. M.; Schaeffer, M. W.; Felker, P. M. *Chem. Phys. Lett.* **1995**, *241*, 603.
(21) Fredericks, S. Y.; Jordan, K. D.; Zwier, T. S. *J. Phys. Chem.* **1996**, *100*, 7810.
(22) Garrett, A. W.; Zwier, T. S. *J. Chem. Phys.* **1992**, *96*, 3402.
(23) Sorenson, J. M.; Gregory, J. K.; Clary, D. C. *J. Chem. Phys.* **1997**, *106*, 849.
(24) Augspurger, J. D.; Dykstra, C. E.; Zwier, T. S. *J. Phys. Chem.* **1993**, *97*, 980.
(25) Felker, P. M. *J. Phys. Chem.* **1992**, *96*, 7844.
(26) Stratton, J. R.; Troxler, T.; Topp, M. R. *Chem. Phys. Lett.* **1994**, *225*, 108.
(27) Troxler, T.; Stratton, J. R.; Smith, P. G.; Topp, M. R. *J. Chem. Phys.* **1994**, 101, 9219.
(28) Stratton, J. R.; Troxler, T.; Pryor, B. A.; Smith, P. G.; Topp, M. R. *J. Phys. Chem.* **1995**, *99*, 1424.
(29) Andrews, P. M.; Pryor, B. A.; Palmer, P. M.; Topp, M. R. *Chem. Phys. Lett.* **1997**, *265*, 224.
(30) Joireman, P. W.; Connell, L. L.; Ohline, S. M.; Felker, P. M. *J. Chem. Phys.* **1992**, *96*, 4118.
(31) Wittmeyer, S. A.; Topp, M. R. *Chem. Phys. Lett.* **1989**, *163*, 261.
(32) Allinger, N. L.; Kok, R. A.; Imam, M. R. *J. Comput. Chem.* **1988**, *9*, 591.
(33) Computational results obtained using software programs from Biosym Technologies of San Diego—graphical displays were printed out from the Insight II molecular modeling system.
(34) Grimme, S.; Löhmannsröben, H.-G. *J. Phys. Chem.* **1992**, *96*, 7005.
(35) Connell, L. L.; Corcoran, T. C.; Joireman, P. W.; Felker, P. M. *J. Phys. Chem.* **1990**, *94*, 1229.
(36) Felker, P. M.; Zewail, A. H. *J. Chem. Phys.* **1987**, *86*, 2460.
(37) Baskin, J. S.; Felker, P. M.; Zewail, A. H. *J. Chem. Phys.* **1987**, *86*, 2483.
(38) Felker, P. M.; Zewail, A. H. *Jet Spectroscopy and Molecular Dynamics*, 1st ed.; Hollas, J. M., Phillips, D., Eds.; Blackie Academic and Professional: Glasgow, 1995; p 181.
(39) Kaziska, A. J.; Wittmeyer, S. A.; Topp, M. R. *J. Phys. Chem.* **1991**, *95*, 3663.
(40) Brooks, B. R.; Bruccoleri, R. E.; Olafson, B. D.; States, D. J.; Swaminathan, S.; Karplus, M. *J. Comput. Chem*. **1983**, *4*, 187.
(41) Nevins, N.; Lii, J.-H.; Allinger, N. L. *J. Comput. Chem.* **1996**, *17*, 695.
(42) Pryor, B. A.; Palmer, P. M.; Andrews, P. M.; Berger, M. B.; Troxler, T.; Topp, M. R. *Chem. Phys. Lett.* **1997**, *271*, 19.
(43) SPARTAN version 4.0. Wavefunction Inc., 18410 Von Karman Ave., #370, Irvine, California 92715.
(44) HyperchemTM. Hypercube Inc., Gainesville, FL.
(45) Cöté, M. J.; Kauffman, J. F.; Smith, P. G.; McDonald, J. D. *J. Chem. Phys.* **1989**, *90*, 2865.
(46) Smith, P. G.; McDonald, J. D. *J. Chem. Phys.* **1990**, *92*, 3991.
(47) Smith, P. G.; Troxler, T.; Topp, M. R. *J. Phys. Chem.* **1993**, *97*, 6983.
(48) Al Rabaa, A.; Le Barbu, K.; Lahmani, F.; Zehnacker-Rentien, A. *J. Phys. Chem.* **1997**, *A101*, 3273.